Society of Medical Education & Research

2021, Volume 1, Page No: 83-96
ISSN: 3108-4826

Journal of Medical Sciences and Interdisciplinary Research

Investigation of the Possible Mechanisms behind Cyclolinopeptides' Anti-Osteoporotic Effects Using Network Pharmacology Analysis

Patrick Andrew Oconnor[1]*, Daniel Thomas Murphy[1], Sean William Kelly[1]

[1]Department of Management, Kemmy Business School, University of Limerick, Limerick, Ireland.

***E-mail** ✉ p.oconnor.ul@yahoo.com

Abstract

Osteoporosis represents a major global health challenge. Cyclolinopeptides (CLPs), which are cyclic hydrophobic peptides derived from flaxseed oil, exhibit antioxidative, immunomodulatory, and antiosteoporotic activities; however, their therapeutic utility in osteoporosis remains insufficiently studied. This study aimed to explore the potential protective effects of CLP-A, CLP-E, and CLP-P in the context of osteoporosis using in vitro models.Potential overlapping targets of CLP-A, CLP-E, and CLP-P with osteoporosis were identified through network pharmacology using databases including GeneCards, DrugBank, DisGeNET, PharmMapper, and BindingDB. Core targets were highlighted via protein–protein interaction (PPI) network analysis in Cytoscape. Cytotoxicity of CLPs was evaluated on MC3T3-E1 and RAW264.7 cells using the CCK-8 assay, while osteogenic differentiation was assessed via alizarin red S staining and alkaline phosphatase (ALP) activity measurement.Network pharmacology analysis indicated that CLP-A, CLP-E, and CLP-P potentially regulate multiple biological processes implicated in osteoporosis, such as signal transduction and positive regulation of transcription from RNA polymerase II promoters, predominantly through pathways linked to cancer, PI3K-Akt signaling, and Ras signaling. In vitro experiments showed that CLPs exhibited no cytotoxicity toward MC3T3-E1 or RAW264.7 cells within 24–48 h. Furthermore, CLP-A, CLP-E, and CLP-P promoted osteogenic differentiation and increased ALP activity in MC3T3-E1 cells.Our findings suggest that CLP-A, CLP-E, and CLP-P enhance osteogenesis and ALP activity in MC3T3-E1 cells without cytotoxic effects, highlighting their promise as antiosteoporotic agents. Network pharmacology analysis further implicates their involvement in critical signaling pathways, including PI3K-Akt and Ras, that are fundamental to bone metabolism and osteoporosis, although further mechanistic studies are warranted.

Keywords: Osteoporosis, Cyclolinopeptides, Signaling pathway, Network pharmacology analysis

Introduction

Osteoporosis is a widespread systemic bone disease characterized by weakened bone structure and heightened fracture risk, affecting roughly 50% of women and one-third of men globally [1]. Fractures of the hip and spine in osteoporotic individuals are associated with substantial morbidity and mortality, with estimates suggesting that 25% of patients over 50 years old who suffer a hip fracture may die within a year [2–4]. Factors including age, sex, and lifestyle strongly influence the development of osteoporosis [2, 3, 5], and recurrent fractures place a considerable burden on both patients and society, significantly impairing quality of life [6].

Bone homeostasis relies on a delicate balance between osteoclast-mediated bone resorption and osteoblast-driven bone formation. Osteoporosis arises when this balance is disrupted, leading to increased bone breakdown relative to formation [7, 8]. In vitro, RAW264.7 cells can differentiate into multinucleated osteoclast-like cells, providing a model for osteoclastogenesis [9, 10]. Hormonal changes,

Access this article online https://smerpub.com/

Received: 15 December 2020; **Accepted:** 19 March 2021

How to cite this article: Oconnor PA, Murphy DT, Kelly SW. Investigation of the Possible Mechanisms behind Cyclolinopeptides' Anti-Osteoporotic Effects Using Network Pharmacology Analysis. J Med Sci Interdiscip Res. 2021;1:83-96. https://doi.org/10.51847/YZp5uBeEmS

particularly reductions in estrogen, directly impact bone cell function and contribute to postmenopausal osteoporosis by favoring bone resorption [5]. Therapeutic strategies often focus on suppressing osteoclast activity using agents such as bisphosphonates, denosumab, or estrogen; however, prolonged inhibition of resorption alone may not effectively enhance bone remodeling [11–13]. Consequently, there is growing interest in treatments that stimulate osteoblast activity to promote bone formation.

Traditional Chinese medicine (TCM) has demonstrated therapeutic benefits across a variety of conditions. Houttuynia cordata Thunb. polysaccharides (HCP) have been shown to modulate gut microbiota [14], while Lonicera japonica Thunb. has historically been used for febrile, gastrointestinal, and inflammatory disorders, and in modern practice for metabolic and infectious diseases, including pneumonia and sepsis [15]. Certain TCM herbs, such as R. rubescens, exhibit anticancer properties with historical usage for pharyngalgia relief [16]. Importantly, TCM has also shown potential in osteoporosis management [17].

Flaxseed (Linum usitatissimum L.) is a major oilseed crop used in TCM [18]. CLPs, cyclic hydrophobic peptides extracted from flaxseed oil, possess diverse pharmacological properties, including antiosteoporotic, antioxidant, and immunomodulatory effects [19–22]. Previous studies have characterized 12 CLP samples via offline MS/MS, confirming purities over 95.5%, composed of 8–9 amino acids and molecular weights around 1 kDa [23]. Given their pharmacological profile, CLPs are promising candidates for osteoporosis therapy [24]. Evidence indicates that flaxseed and flax oil can mitigate estrogen-deficiency-induced osteoporosis by reducing osteoclast activity [25, 26], and flax extracts help preserve bone mass and strength in postmenopausal osteoporosis models [27]. Despite this, research on CLPs specifically as antiosteoporotic agents remains limited.

In this study, we applied network pharmacology to predict potential osteoprotective effects of CLP-A, CLP-E, and CLP-P, followed by experimental validation of their antiosteoporotic activity in vitro.

Materials and Methods

Network pharmacology

Identification of cyclolinopeptide targets

The chemical structures of CLP-A, CLP-E, and CLP-P were retrieved from the SciFinder database (https://scifinder-n.cas.org/). Canonical SMILES were obtained and converted into three-dimensional structures using Chem3D 20.0 software. Structures underwent energy minimization via the MM2 method and were subsequently saved in the mol2 format. Potential targets of CLP-A, CLP-E, and CLP-P were predicted by submitting their structures to the PharmMapper database (http://www.lilab-ecust.cn/pharmmapper/) and the BindingDB database (http://www.bindingdb.org/bind/index.jsp), while canonical SMILES were submitted to the SuperPred platform (https://prediction.charite.de/). To enhance the reliability of results, the BindingDB "Similarity" threshold was set at a minimum of 0.85. All retrieved targets were standardized and unified using the UniProt database (https://www.uniprot.org).

Collection of osteoporosis-related targets

Targets associated with osteoporosis were retrieved from GeneCards (https://www.genecards.org), DrugBank (https://go.drugbank.com), and DisGeNET (https://www.disgenet.org). The targets were standardized via UniProt, duplicates were removed, and the datasets were merged for downstream analysis.

Protein-Protein Interaction (PPI) network construction and core target screening

To identify intersections between CLP-related and osteoporosis-related targets, the datasets were analyzed using Venny 2.1.0 (https://bioinfogp.cnb.csic.es/tools/venny/), and Venn diagrams were generated to visualize overlapping targets. The shared targets were uploaded to the STRING database (https://cn.string-db.org/) with "Homo sapiens" selected as the species, a minimum interaction score of 0.7, and unconnected nodes hidden. The resulting PPI network was exported as a TSV file and analyzed using Cytoscape software, employing Network Analyzer and CytoNCA plugins. Core targets were defined as those with a degree value exceeding twice the network median.

Gene Ontology (GO) and KEGG pathway enrichment analysis

Overlapping targets of CLPs and osteoporosis were imported into DAVID Bioinformatics Resources (https://david.ncifcrf.gov/) for functional annotation via GO enrichment and KEGG pathway analysis, with species limited to "Homo sapiens." Terms with $P < 0.05$ were considered significant, and the top 20 enriched

terms were visualized using an online bioinformatics platform (http://www.bioinformatics.com.cn/).

Pharmacological experiments in vitro

Cell culture

RAW264.7 cells (Procell CL-0190, Wuhan Procell Life Technology Co., Ltd.) and MC3T3-E1 cells (Procell CL-0378, Wuhan Procell Life Technology Co., Ltd.) were maintained in MEM-ALPHA medium supplemented with 10% fetal bovine serum (FBS), 1 percent penicillin, and 1 percent streptomycin at 37 °C in a humidified atmosphere containing 5% CO2.

Cell proliferation and cytotoxicity assay

Cell viability and proliferation were assessed using the Cell Counting Kit-8 (CCK-8, DOJINDO, Japan) following the manufacturer's instructions. MC3T3-E1 and RAW264.7 cells were seeded in 96-well plates at a density of 1×10^4 cells/well and incubated overnight. Once cells reached 70–80% confluency, MC3T3-E1 cells were divided into the following groups: control, estrogen (E2, positive control), CLP-A, CLP-E, CLP-P, high-concentration cyclosporin A (CsA, 1 μg/mL), and low-concentration CsA (0.1 μg/mL). CLP-A, CLP-E, and CLP-P were provided by Professor Yong Wang (Guangdong Saskatchewan Oilseed Joint Laboratory, Department of Food Science and Engineering, Jinan University, Guangzhou, China).

For osteogenic differentiation, MC3T3-E1 cells were treated with osteogenic induction medium (1 μg/mL) or respective compounds, with medium replacement every 2–3 days until day 8. Osteogenic differentiation was induced using complete medium supplemented with ascorbic acid (50 μg/mL) and sodium β-glycerophosphate (10 mM), while the control group received FBS-free MEM-ALPHA medium.

CCK-8 assay for cell viability

On day 9, 10 μL of CCK-8 solution was added to each well and incubated for 2 h in the dark. Absorbance was measured at 450 nm using a SYNERGY H1 microplate reader (BioTek, USA) to assess cell proliferation and cytotoxicity.

Assessment of osteogenic differentiation and alizarin red s staining in MC3T3-E1 cells

MC3T3-E1 cells were assigned to eight experimental groups: negative control (no osteogenic medium), standard control (osteogenic medium only), vehicle control (1% absolute ethanol), 10 nM estrogen (E2), CLP-A, CLP-E, CLP-P, and Secoisolariciresinol diglucoside (SDG). Osteogenic differentiation was evaluated using the Alizarin Red S staining kit (Beyotime) according to the manufacturer's instructions. Cells were plated at 1 × 10^5 cells per well in 12-well plates. Mineralized nodule formation was induced in all groups except the negative control by refreshing the medium with osteogenic differentiation medium. The control group received only differentiation medium, whereas the vehicle group included 1% ethanol. Treatment concentrations were set at 10 nM for E2 and 0.1 μg/mL for each cyclolinopeptide. Cultures were maintained for 30 days, with medium replacement every 2–3 days until visible osteogenic differentiation was achieved.

After the treatment period, cells were rinsed twice with PBS and fixed in 4% paraformaldehyde for 15 minutes. Alizarin Red S staining solution was applied for 10 minutes at room temperature (25 °C), followed by rinsing with double-distilled water. Stained mineral deposits were captured using an upright microscope (OLYMPUS, Japan). For quantitative assessment, 0.5 M HCl containing 5% SDS was added to each well, incubated for 30 minutes, and 200 μL of the solution was transferred to a 96-well plate. Absorbance at 415 nm was measured using a SYNERGY H1 microplate reader (BioTek, USA).

Alkaline Phosphatase (ALP) staining and quantification

For ALP evaluation, MC3T3-E1 cells were cultured in α-MEM supplemented with 10% FBS, 1% penicillin/streptomycin, 10 mM β-glycerophosphate, and 50 μg/mL ascorbic acid for seven days, with medium replaced every two days. On day eight, cells were washed twice with PBS and fixed in 4% paraformaldehyde for 10 minutes. ALP activity was determined using the Sainto-bio ALP staining kit (Shanghai, China). Cells were incubated with ALP reagent for 20 minutes under light-protected conditions and counterstained with methyl green for 3–5 minutes. Imaging was performed with an upright microscope (OLYMPUS, Japan), and staining intensity was used as a semi-quantitative measure of ALP activity. ImageJ software was employed for quantification.

Statistical analysis

All assays were repeated at least three times independently. Data were analyzed and visualized using GraphPad Prism (GraphPad Software, Inc., USA).

Results and Discussion

Target identification via network pharmacology

Using PharmMapper, BindingDB, and SuperPred, 420, 399, and 410 potential molecular targets were predicted for CLP-A, CLP-E, and CLP-P, respectively. Following the removal of duplicates, 487 unique targets were obtained for further analysis.

Screening of osteoporosis-related targets and overlap analysis

Osteoporosis-associated targets were retrieved from GeneCards (4959), DrugBank (205), and DisGeNET (1098). After merging datasets and eliminating redundancies, 5315 distinct targets were obtained. Venn diagram analysis revealed the overlap between CLP-related targets and osteoporosis-associated targets, highlighting potential molecular intersections through which CLPs may exert antiosteoporotic effects **(Figure 1).**

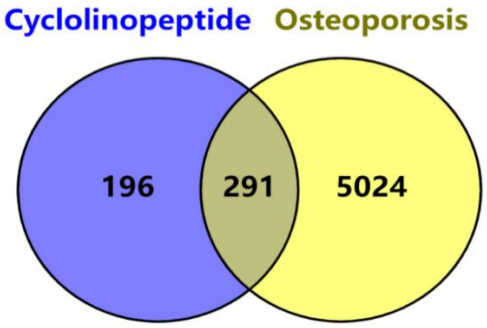

Figure 1. Overlapping targets between cyclolinopeptides and osteoporosis

Protein-Protein Interaction (PPI) network analysis

Interactions among the overlapping targets were evaluated using the STRING database, resulting in the construction of a PPI network. After removing unconnected nodes, the network comprised 291 nodes and 1249 edges **(Figure 2)**. The median degree of nodes in the network was 12, and targets with a degree value at least twice the median were designated as key nodes. Using this criterion, 71 core targets were identified, which are listed in **Table 1** and visualized in **Figure 3.**

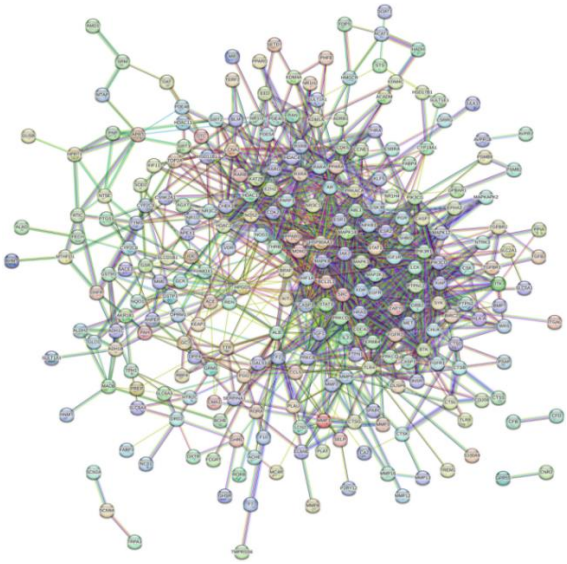

Figure 2. Protein-Protein Interaction (PPI) network

Table 1. Core targets of cyclolinopeptides acting on osteoporosis (Ranked by node degree)

No.	Gene Symbol	Function / Gene Name	No.	Gene Symbol	Function / Gene Name
1	SRC	Proto-oncogene SRC	37	KIT	Stem cell factor receptor
2	MAPK1	Mitogen-activated protein kinase 1	38	PGR	Progesterone receptor
3	STAT3	Signal transducer and activator of transcription 3	39	BTK	Bruton tyrosine kinase
4	MAPK1	Mitogen-activated protein kinase 1	40	ABL1	Abelson tyrosine kinase 1
5	PIK3R1	Phosphatidylinositol-4,5-bisphosphate 3-kinase regulatory subunit 1	41	CDK2	Cyclin-dependent kinase 2
6	EGFR	Epidermal growth factor receptor	42	BTK	Bruton tyrosine kinase
7	HRAS	Harvey rat sarcoma viral oncogene homolog	43	ZAP70	T cell receptor signaling kinase
8	GRB2	Growth factor receptor-bound protein 2	44	SYK	Spleen tyrosine kinase

9	ESR1	Estrogen receptor 1	45	MET	Hepatocyte growth factor receptor
10	PTPN11	Protein tyrosine phosphatase, non-receptor type 11	46	RARA	Retinoic acid receptor alpha
11	HDAC1	Histone deacetylase 1	47	PRKCB	Protein kinase C beta
12	IGF1	Insulin-like growth factor 1	48	EZH2	Enhancer of zeste homolog 2
13	JAK2	Janus kinase 2	49	KAT2B	Histone acetyltransferase 2B
14	LCK	Lymphocyte-specific protein tyrosine kinase	50	KIT	Stem cell factor receptor
15	MAPK8	Mitogen-activated protein kinase 8	51	NOS3	Nitric oxide synthase 3
16	MAPK14	Mitogen-activated protein kinase 14	52	PGR	Progesterone receptor
17	RXRA	Retinoid X receptor alpha	53	ERBB4	V-Erythroblastoid murine leukemia viral oncogene homolog 4
18	AR	Androgen receptor	54	ESR2	Estrogen receptor beta
19	STAT1	Signal transducer and activator of transcription 1	55	PTPN1	Protein tyrosine phosphatase, non-receptor type 1
20	HIF1A	Hypoxia-inducible factor 1 alpha	56	F2	Coagulation factor II
21	ALB	Albumin	57	PARP1	Poly (ADP-ribose) polymerase 1
22	NFKB1	Nuclear factor kappa B 1	58	CSK	C-src inhibitory protein
23	CASP3	Caspase 3	59	NOS2	Inducible nitric oxide synthase
24	MAP2K1	Mitogen-activated protein kinase kinase 1	60	RXRB	Retinoid X receptor beta
25	TLR4	Toll-like receptor 4	61	PRKCQ	Protein kinase C theta
26	HPGDS	2',3'-dihydroxypropyl coenzyme A dihydrogenase	62	CCNA2	Cyclin A2
27	PIK3CD	Phosphatidylinositol-4,5-bisphosphate 3-kinase catalytic delta	63	PPARA	Peroxisome proliferator-activated receptor alpha
28	PRKACA	Protein kinase A catalytic subunit alpha	64	RARB	Retinoic acid receptor beta
29	KDR	Kinase insert domain receptor	65	MMP2	Matrix metallopeptidase 2
30	PPARG	Peroxisome proliferator-activated receptor gamma	66	ITK	Interleukin-2 inducible T-cell kinase
31	NR3C1	Nuclear receptor subfamily 3 group C member 1	67	GSK3B	Glycogen synthase kinase 3 beta
32	IGF1R	Insulin-like growth factor 1 receptor	68	RARG	Retinoic acid receptor gamma
33	MDM2	E3 ubiquitin-protein ligase MDM2	69	FGFR2	Fibroblast growth factor receptor 2
34	MMP9	Matrix metallopeptidase 9	70	THRB	Thyroid hormone receptor beta
35	HDAC2	Histone deacetylase 2	71	MAPK12	Mitogen-activated protein kinase 12
36	SRC	Proto-oncogene SRC			

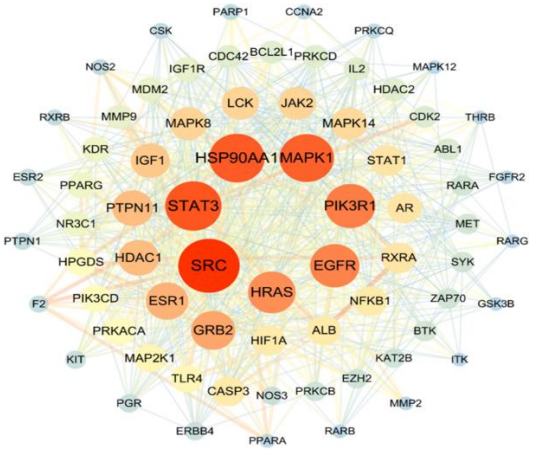

Figure 3. Core target interaction network (Node size corresponds to degree value)

Gene Ontology (GO) and KEGG pathway enrichment analysis

The 76 identified core targets were subjected to GO and KEGG enrichment analysis using the DAVID database. GO analysis encompassed both biological processes (BP) **(Figure 4)** and molecular functions (MF) **(Figure 5)**, with darker colors representing lower P-values. KEGG pathway analysis was performed to elucidate the potential molecular mechanisms underlying the anti-osteoporotic effects of cyclolinopeptides (CLPs). The analysis highlighted pathways including PI3K-Akt

signaling, Ras signaling, lipid and atherosclerosis, chemical carcinogenesis—receptor activation, hepatitis B, thyroid hormone signaling, endocrine resistance, estrogen signaling, and resistance to EGFR tyrosine kinase inhibitors **(Figure 6).**

As depicted in **Figure 7,** both the PI3K-Akt and estrogen signaling pathways regulate key cellular processes such as apoptosis, proliferation, survival signaling, and signal transduction, which are intimately linked to osteoporosis development and progression. The reference for **Figure 7** regarding these pathways was obtained from DAVID Bioinformatics Resources, and the figures were prepared using PowerPoint 2016.

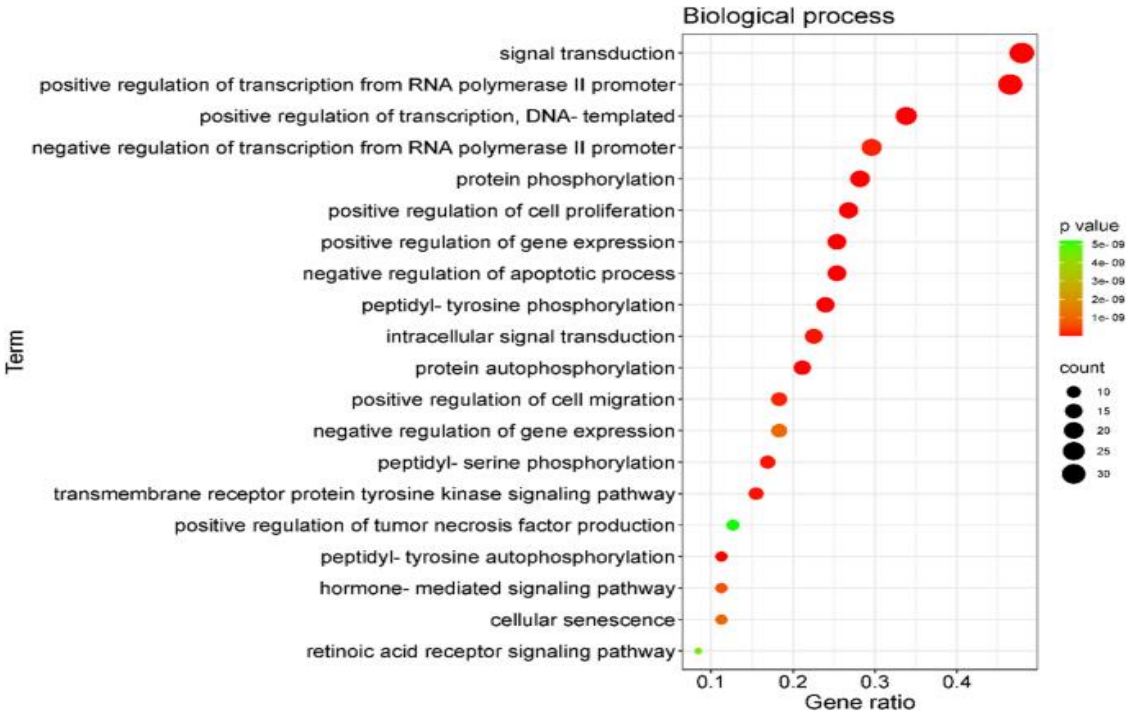

Figure 4. Biological process analysis of core targets

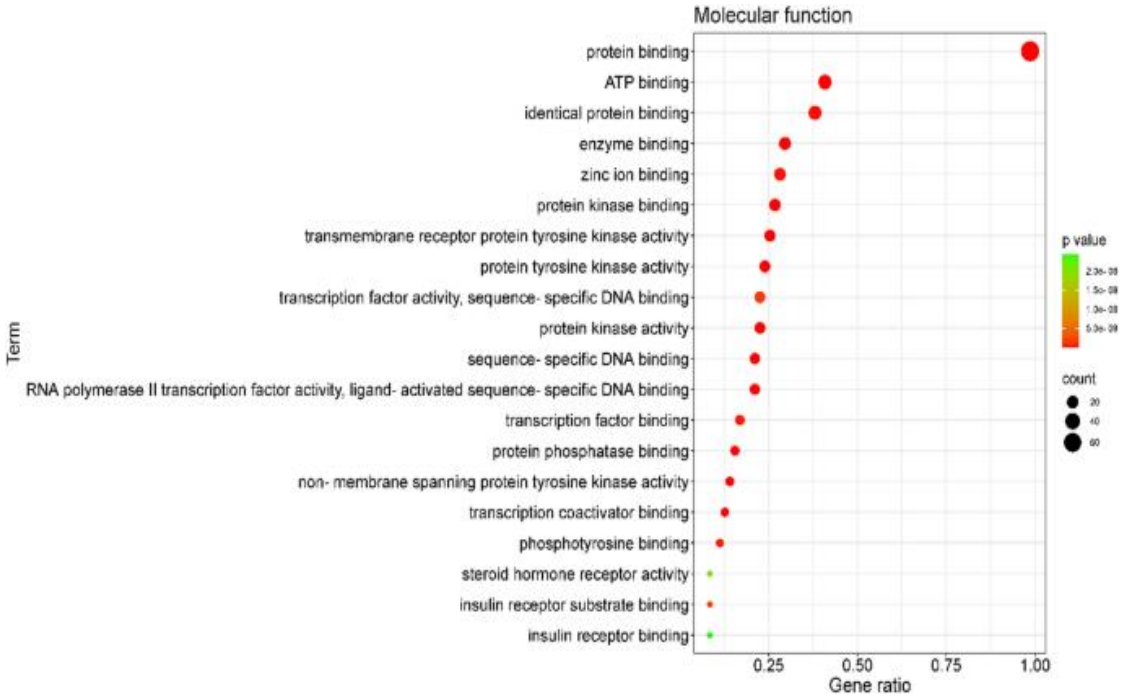

Figure 5. Molecular Function (MF) analysis of the core targets

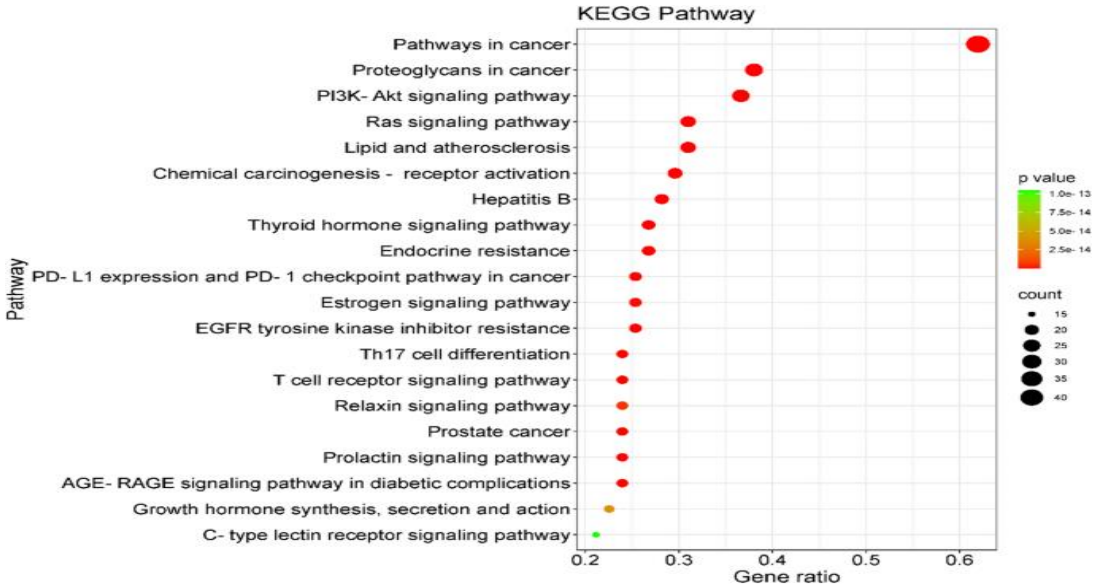

Figure 6. KEGG pathway analysis of core targets

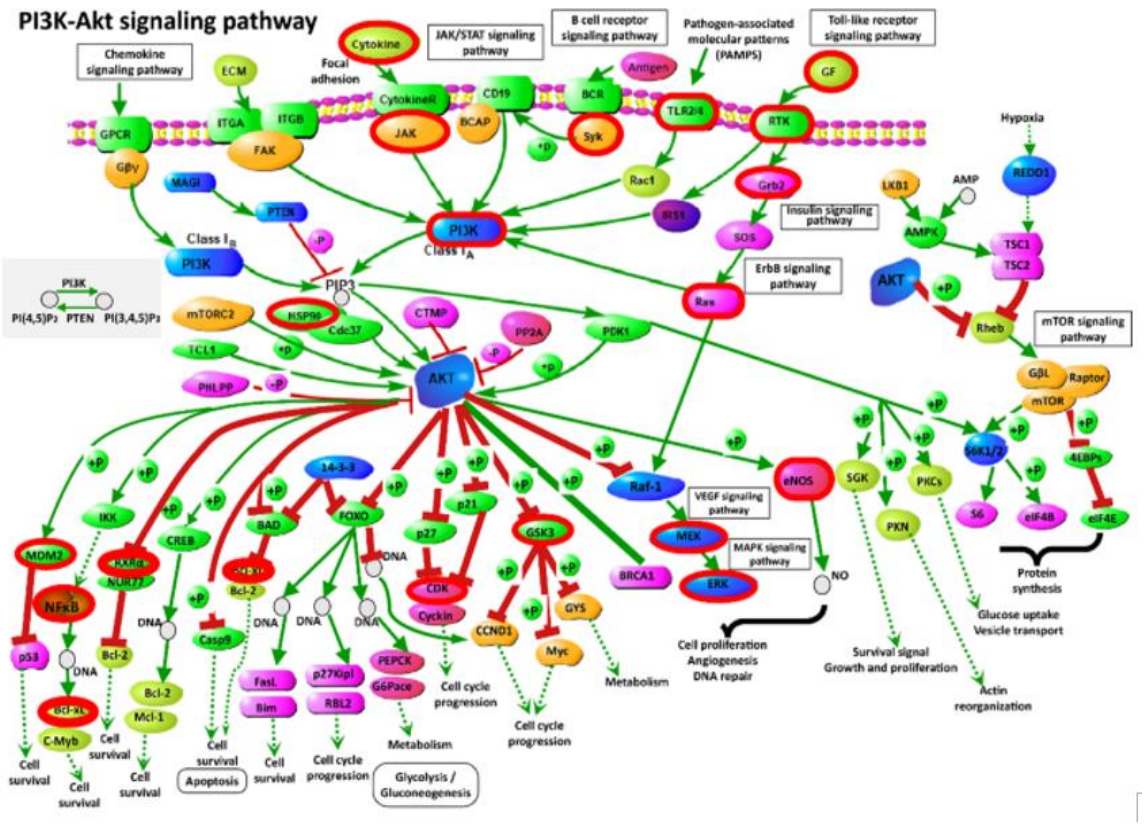
PI3K-Akt signaling pathway
Chemokine signaling pathway
ECM
Focal adhesion
Cytokine
JAK/STAT signaling pathway
B cell receptor signaling pathway
Pathogen-associated molecular patterns (PAMPS)
Toll-like receptor signaling pathway
Antigen
GF
GPCR
ITGA
ITGB
FAK
CytokineR
JAK
CD19
BCAP
BCR
Syk
TLR2/4
RTK
Hypoxia
REDD1
Gβγ
MAGI
PTEN
PI3K
Class IA
Class IB
PIP3
Rac1
Grb2
IRS1
SOS
Insulin signaling pathway
LKB1
AMP
AMPK
TSC1
TSC2
AKT
Rheb
mTOR signaling pathway
ErbB signaling pathway
Ras
mTORC2
HSP90
Cdc37
CTMP
PP2A
PDK1
TCL1
PHLPP
Gβ L
Raptor
mTOR
4EBPs
eIF4E
S6K1/2
S6
eIF4B
Protein synthesis
Glucose uptake
Vesicle transport
Actin reorganization
Survival signal
Growth and proliferation
PKCs
PKN
SGK
eNOS
NO
Cell proliferation
Angiogenesis
DNA repair
Raf-1
VEGF signaling pathway
MEK
ERK
MAPK signaling pathway
BRCA1
Metabolism
GSK3
GYS
Myc
CCND1
Cell cycle progression
CDK
Cyclin
p21
p27
14-3-3
FOXO
BAD
Bcl-2
Casp9
FasL
Bim
p27Kipl
RBL2
PEPCK
G6Pace
Metabolism
Glycolysis / Gluconeogenesis
Cell survival
Apoptosis
IKK
CREB
MDM2
HXRα
NUR77
NFκB
p53
c-Myb
bcl-xL
Mcl-1
DNA
+P
-P

a)

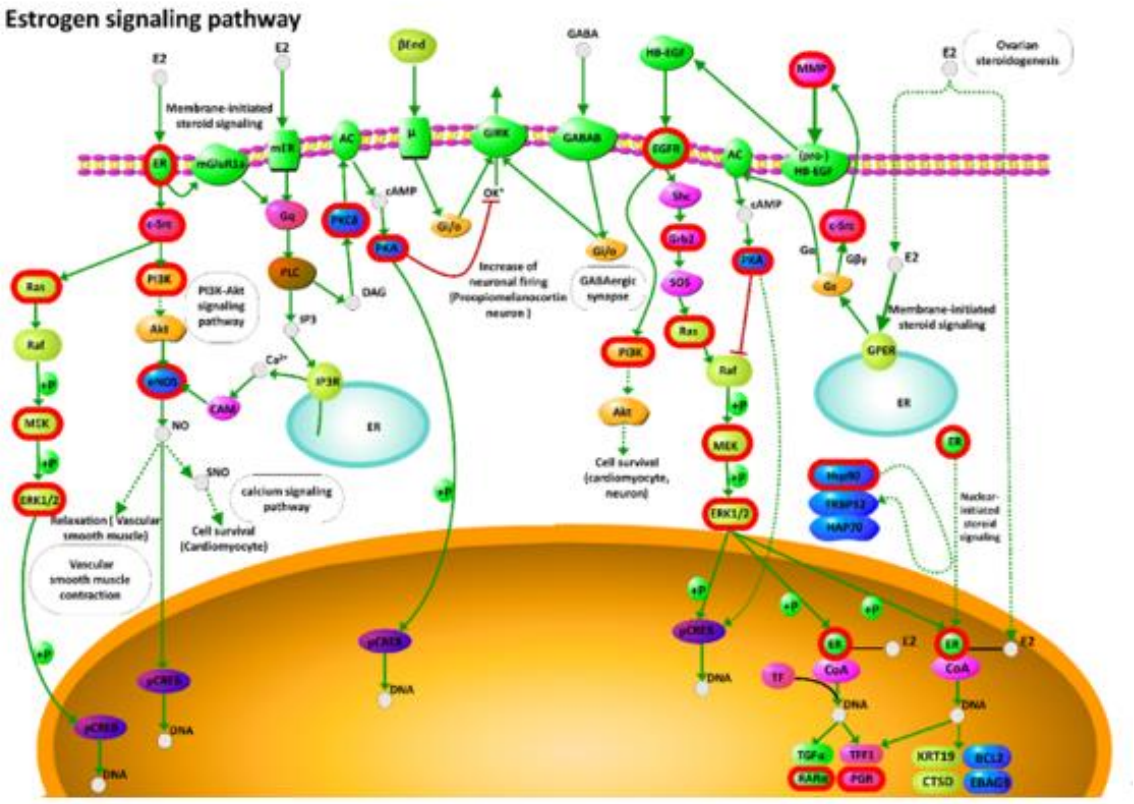

b)

Figure 7. Key signaling pathways involved in osteogenesis and the potential anti-osteoporosis effects of cyclolinopeptides. **a)** PI3K-Akt signaling pathway. **b)** Estrogen signaling pathway. (Source: Huamei CUSABIO technical team, used with permission)

Pharmacodynamic study

Impact of cyclolinopeptides (CLPs) on MC3T3-E1 cell proliferation and cytotoxicity

Exposure of MC3T3-E1 cells to CLP-A for 24 or 48 hours resulted in a notable reduction in cell viability at concentrations above 199.05 × 10^{-1} μg/mL **(Figure 8a)**. The IC_{50} value for 24-hour treatment was calculated as 401.4 × 10^{-1} μg/mL. For CLP-E, the IC_{50} values after 24 and 48 hours of exposure were 19.24 × 10^{-1} μg/mL and 10.91 × 10^{-1} μg/mL, respectively **(Figure 8b)**. Treatment with CLP-P and secoisolariciresinol diglucoside (SDG) for 48 hours yielded IC_{50} values of 425.1 × 10^{-1} μg/mL and 179.6 × 10^{-1} μg/mL, respectively **(Figure 8c)**, while the IC_{50} for CLP-P after 24 hours was 417.4 × 10^{-1} μg/mL **(Figure 8d).**

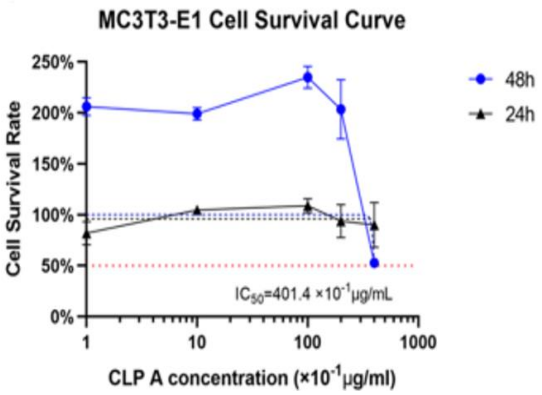

a)

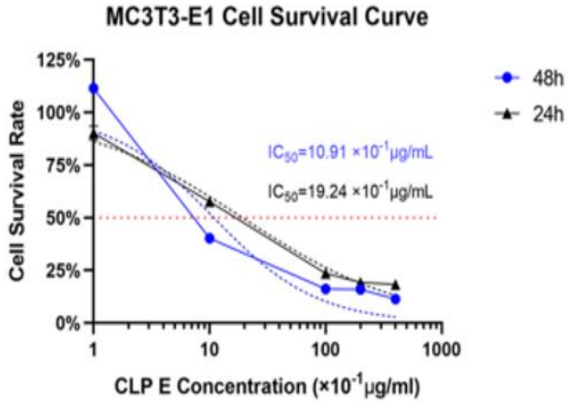

b)

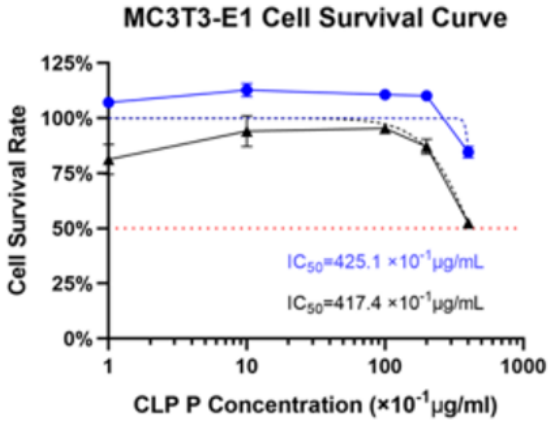

c)

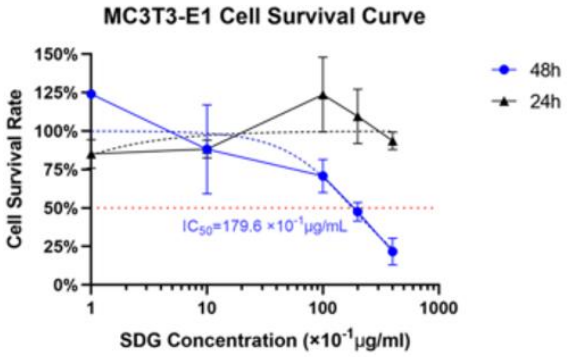

d)

Figure 8. MC3T3-E1 cell proliferation and cytotoxicity

Effects of cyclolinopeptides (CLPs) on RAW264.7 cell proliferation and cytotoxicity

A CCK-8 assay revealed that exposure of RAW264.7 cells to CLP-A for twenty four or forty eight hours yielded IC_{50} values of 264.9 × 10^{-1} μg/mL and 261.5 × 10^{-1} μg/mL, respectively. As illustrated in **Figure 9**, CLP-E exhibited no notable toxicity toward RAW264.7 cells at concentrations below 1 μg/mL. However, cell viability markedly declined at CLP-E concentrations exceeding 1 μg/mL. The IC_{50} values following 24-hour and 48-hour treatments with CLP-E were 34.71 × 10^{-1} μg/mL and 34.29 × 10^{-1} μg/mL, respectively. Treatment of RAW264.7 cells with CLP-P or secoisolariciresinol diglucoside (SDG) at concentrations below 100 μg/mL for twenty four or forty eight hours did not result in any significant reduction in cell viability.

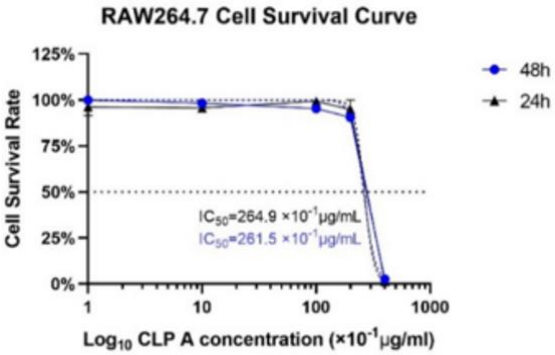

RAW264.7 Cell Survival Curve

a)

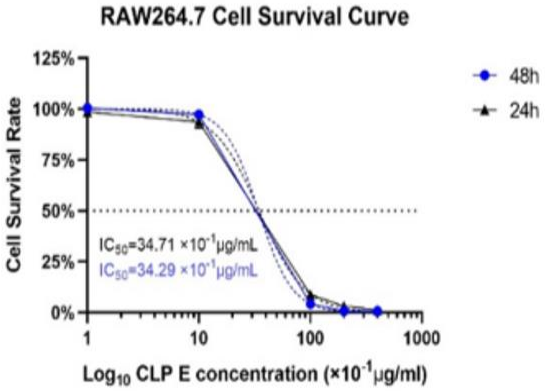

b)

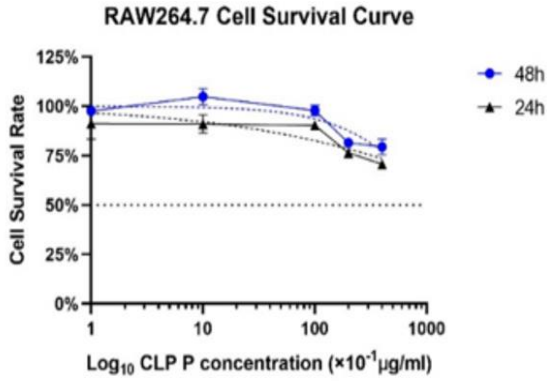

c)

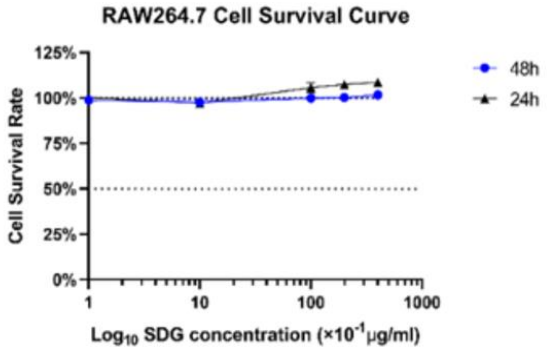

d)

Figure 9. RAW264.7 cell proliferation and cytotoxicity

Effects of cyclolinopeptides (CLPs) on osteoblasts

The impact of CLPs on osteoblasts was evaluated. As depicted in **Figure 10**, treatment with CLP-A (0.1 µg/mL), CLP-E (0.1 µg/mL), CLP-P (0.1 µg/mL), secoisolariciresinol diglucoside (SDG), or estradiol (E2) resulted in increased alizarin red S (ARS) staining and a higher mineralization rate compared to the control group. These findings suggest that these compounds exert a promoting effect on osteoblast activity.

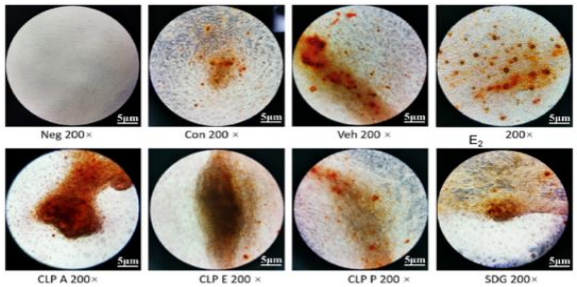

a)

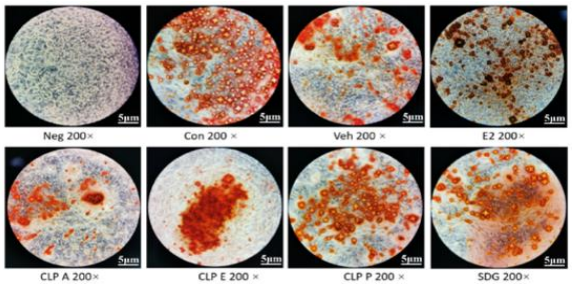

b)

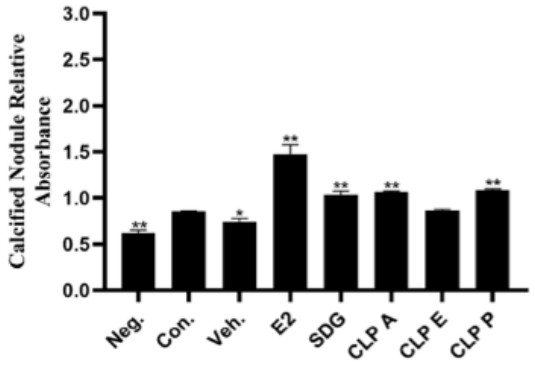

c)

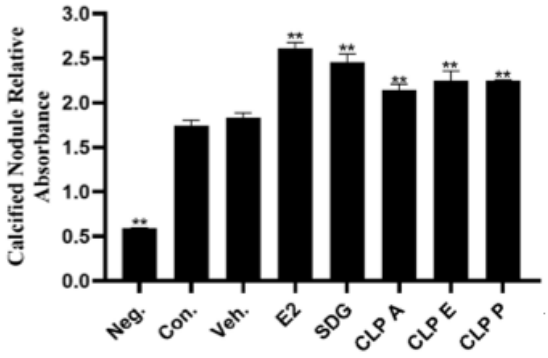

d)

Figure 10. Absorbance values indicating the effects of various compounds on mineralized nodule formation in pre-osteoblasts. **a and c** Medium changed every 2 days. **b and d** Medium changed every three days (MC3T3-E1 cells). Values are expressed as means ± S.E.M.; differences compared to control are marked as *P < 0.05, **P < 0.01.

Effects of cyclolinopeptides (CLPs) on alkaline phosphatase (ALP) activity in osteoblasts

As presented in **Figures 11a and 11b**, ALP activity in MC3T3-E1 cells decreased after treatment with CLP-A or E2. However, lower concentrations of CLP-A produced higher ALP activity than did higher concentrations.

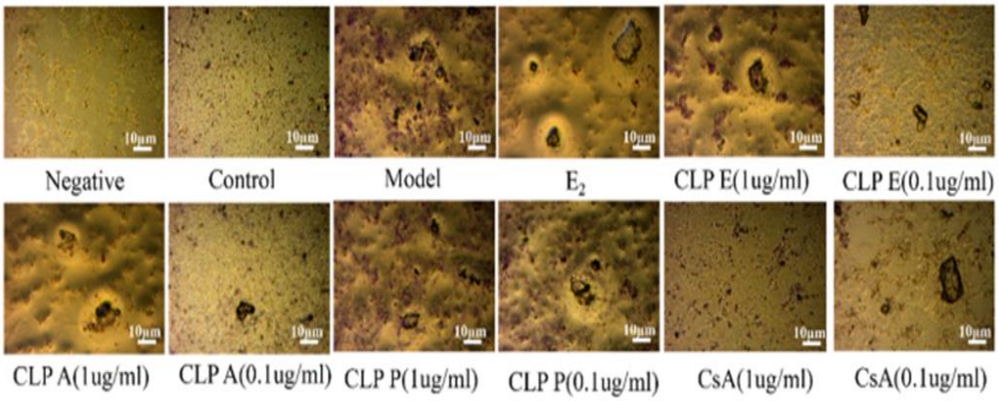

a)

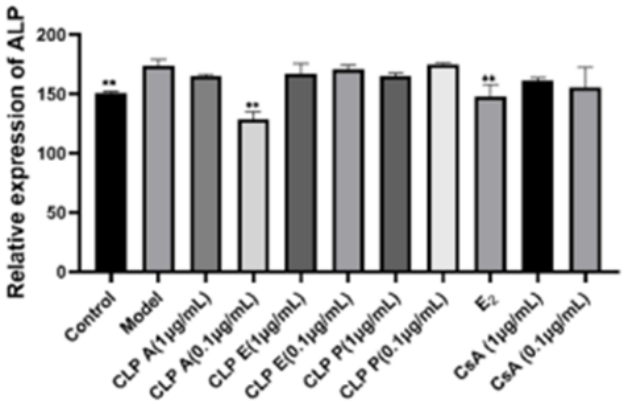

b)

Figure 11. Alkaline phosphatase (ALP) staining in MC3T3-E1 cells. A Visual staining for alkaline phosphatase activity. B Quantitative analysis of alkaline phosphatase activity (MC3T3-E1 cells). Data are shown as means ± S.E.M.; significant differences relative to the Model group: **P < 0.005.

Osteoporosis continues to pose a serious global health threat. Prior research has indicated that it causes over 1.6 million fractures annually [28]. Chronic bone pain substantially reduces patients' quality of life, and osteoporosis remains the leading cause of skeletal complications. Recent studies have established that the condition arises from disrupted bone metabolism, resulting in excessive bone loss [28]. Bone remodeling maintains equilibrium through a balance where osteoblast-mediated bone formation offsets osteoclast-driven resorption, thereby preserving steady bone mass. However, as osteoblast function declines, support for counteracting osteoclastic resorption weakens, leading to bone density reduction of various origins and eventually progressing to osteoporosis [29]. Effective management of osteoporosis therefore depends on enhancing osteoblast activity.

Osteogenesis involves the proliferation of pre-osteoblasts, their differentiation into mature osteoblasts, and the subsequent production of a collagen-rich extracellular matrix (ECM). This process begins with rapid proliferation of undifferentiated cells, followed by growth cessation and ECM deposition. Matrix synthesis then activates early markers of osteoblast differentiation, such as alkaline phosphatase (ALP), which initiates mineralization of the collagen ECM through calcium and phosphate deposition [30]. The MC3T3-E1 cell line serves as a well-established model exhibiting pre-osteoblast characteristics, while cyclolinopeptides (CLPs) are cyclic peptides known to suppress osteoclast differentiation [31]. Notably, CLP-F inhibits RANKL-induced osteoclast formation by downregulating RANK expression [32]. In this investigation, CLP-A, CLP-E, and CLP-P enhanced ALP activity and promoted a higher mineralization rate in MC3T3-E1 pre-osteoblasts

cultured in osteogenic differentiation medium. Overall, these compounds—CLP-A, CLP-E, and CLP-P—demonstrated the ability to boost osteogenic activity.

Network pharmacology predictions in this study identified key targets of CLP-A, CLP-E, and CLP-P in osteoporosis treatment, including SRC, STAT3, HSP90AA1, MAPK1, PIK3R1, EGFR, HRAS, GRB2, ESR1, PTPN11, HDAC1, IGF1, JAK2, LCK, and MAPK8. Gene Ontology (GO) enrichment analysis highlighted that the main biological processes influenced by these CLPs in managing osteoporosis encompass signal transduction regulation, positive regulation of RNA polymerase II-dependent transcription, transcriptional control, protein phosphorylation, and positive modulation of cell proliferation, among others. Extensive evidence supports the critical role of signal transduction regulation in osteoporosis therapy, including modulation of the TGF-beta/Smad pathway [28] and the SIRT1 and PI3K/AKT/mTOR pathways [33] to enhance osteoblast survival. Additionally, increased phosphorylation of the AMP-activated protein kinase α subunit (AMPKα) and activation of the AMPK/Smad1 pathway can drive osteoblast differentiation and effectively stimulate bone formation in vivo [11]. Strategies that promote osteoblast proliferation while suppressing apoptosis are likely to play a key role in preventing osteoporosis [34].

The targets showed enrichment in several key molecular functions, such as protein-protein interactions, adenosine triphosphate (ATP) binding, homodimerization, interactions with enzymes, zinc ion coordination, kinase interactions, and receptor tyrosine kinase activity across cell membranes. Bone-forming cells (osteoblasts) produce and release the cytokine macrophage colony-stimulating factor (M-CSF), which engages its receptor (CSF1R or C-FMS) on bone-resorbing cells (osteoclasts) and monocyte/macrophage precursors—a vital step in osteoclast development [35]. The ATP-binding cassette transporter g1 also has a significant function in modulating bone formation processes [36].

These targets were chiefly located in subcellular structures like the cell nucleus, cytoplasm, soluble cytosol, nuclear interior, cell membrane, and large protein assemblies. Damage to DNA from oxidative stress in the nucleus, along with programmed cell death and cell aging, can drive impaired tissue function and disrupt the balance of bone remodeling in cytoplasmic compartments [37].

Pathway analysis via KEGG highlighted several candidate routes, including the PI3K-Akt pathway, Ras pathway, lipids in atherosclerosis, receptor-mediated chemical carcinogenesis, hepatitis B-related signaling, thyroid hormone regulation, resistance to endocrine therapies, estrogen-mediated signaling, and resistance to EGFR tyrosine kinase inhibitors.

A lack of estrogen impacts cellular commitment and cell death, speeds up bone remodeling rates, and boosts excessive bone breakdown, ultimately causing osteoporosis. Estrogen can activate bone morphogenetic protein (BMP) pathways, encouraging mesenchymal stem cells to commit to bone-forming lineages instead of adipocytes [38]. Blocking the PI3K/AKT route aggravates the maturation of both bone-forming and bone-resorbing cells, thereby triggering osteoporosis [39]. In contrast, stimulating PI3K/Akt signaling alongside red blood cell production in the marrow can protect against bone loss in osteoporosis by stimulating new vessel growth and specialized (H-type) vascular formation [40].

The present work, using network pharmacology approaches, uncovered that the PI3K-Akt and estrogen pathways likely underlie the beneficial mechanisms of CLP-A, CLP-E, and CLP-P against osteoporosis. Cell culture experiments confirmed that these compounds stimulated bone formation and boosted alkaline phosphatase (ALP) levels.

Conclusion

To summarize, this research established the strong cell-based therapeutic promise of cyclolinopeptides (CLP-A, CLP-E, and CLP-P) isolated from flaxseed oil in combating osteoporosis. They augmented bone-building activity and raised ALP levels in MC3T3-E1 cells with no evidence of cell toxicity, indicating their candidacy as novel treatments for the condition. Bioinformatic network analysis points to their beneficial effects being mediated mainly via estrogen and PI3K-Akt pathways, possibly through modulation of proteins like SRC, STAT3, HSP90AA1, MAPK1, PIK3R1, and EGFR. This work supports CLP-A, CLP-E, and CLP-P as effective compounds for osteoporosis management. Thus, additional confirmation of their anti-osteoporosis mechanisms is warranted in ongoing studies by our team. Although encouraging, the results are restricted to cell-based experiments and require animal model testing for validation. Subsequent investigations should delve into

detailed pathway interactions, assess absorption/distribution profiles, and evaluate safety in animal studies. Teamwork across disciplines will be vital to develop cyclolinopeptide therapies for osteoporosis, highlighting the importance of thorough animal and human trials to fully utilize their clinical value.

Acknowledgments: None

Conflict of Interest: None

Financial Support: None

Ethics Statement: None

References

1. Wu D, et al. T-cell mediated inflammation in postmenopausal osteoporosis. Front Immunol. 2021. https://doi.org/10.3389/fimmu.2021.687551.
2. Ensrud KE, Crandall CJ. Osteoporosis Annals Intern Med. 2017;167(3):ITC17–32.
3. Gkastaris K, et al. Obesity, osteoporosis and bone metabolism. J Musculoskelet Neuronal Interact. 2020;20(3):372–81.
4. Słupski W, Jawień P, Nowak B. Botanicals in postmenopausal osteoporosis. Nutrients. 2021. https://doi.org/10.3390/nu13051609.
5. Aspray TJ, Hill TR. Osteoporosis and the ageing skeleton. Biochemistry and cell biology of ageing: part II clinical science. Springer Singapore: Singapore; J.R. Harris and V.I. Korolchuk, Editors. 2019;453–76.
6. Lim SY. Romosozumab for the treatment of osteoporosis in women: efficacy, safety, and cardiovascular risk. Womens Health. 2022;18:17455057221125577.
7. Eastell R, Szulc P. Use of bone turnover markers in postmenopausal osteoporosis. Lancet Diabetes Endocrinol. 2017;5(11):908–23.
8. Marcucci G, Brandi ML. The diagnosis and therapy of osteoporosis in Gaucher disease. Calcif Tissue Int. 2025;116(1):31.
9. Boyce BF. Advances in the regulation of osteoclasts and osteoclast functions. J Dent Res. 2013;92(10):860–7.
10. Kong L, Smith W, Hao D. Overview of RAW264.7 for osteoclastogensis study: phenotype and stimuli. J Cell Mol Med. 2019;23(5):3077–87.
11. Zhang F, et al. Anti-osteoporosis activity of sanguinarine in preosteoblast MC3T3-E1 cells and an ovariectomized rat model. J Cell Physiol. 2018;233(6):4626–33.
12. Kanis JA, et al. Executive summary of European guidance for the diagnosis and management of osteoporosis in postmenopausal women. Aging Clin Exp Res. 2019;31(1):15–7.
13. Kendler D, et al. Bone mineral density after transitioning from denosumab to alendronate. J Clin Endocrinol Metabolism. 2020;105(3):e255–64.
14. Gao S, et al. Unveiling polysaccharides of *houttuynia cordata* Thunb.: extraction, purification, structure, bioactivities, and structure–activity relationships. Phytomedicine. 2025;138:156436.
15. Gao S, et al. *Rabdosia rubescens* (Hemsl.) H. Hara: a potent anti-tumor herbal remedy — botany, phytochemistry, and clinical applications and insights. J Ethnopharmacol. 2025;340:119200.
16. Gao S, et al. Polysaccharides from lonicera Japonica Thunb.: Extraction, purification, structural features and biological activities—A review. Int J Biol Macromol. 2024;281:136472.
17. Lin J, et al. Chinese single herbs and active ingredients for postmenopausal osteoporosis: from preclinical evidence to action mechanism. Biosci Trends. 2017;11(5):496–506.
18. Ramin A, Mohammad MZ, Amir HD. A review on Pharmacological and clinical aspects of Linum usitatissimum L. Curr Drug Discov Technol. 2019;16(2):148–58.
19. Shim YY, et al. Health benefits of flaxseed and its peptides (linusorbs). Crit Rev Food Sci Nutr. 2024;64(7):1845–64.
20. Zheng H, et al. Mechanisms and structure-activity relationships of natural polysaccharides as potential anti-osteoporosis agents: a review. Int J Biol Macromol. 2025;298:139852.
21. Chen J, et al. Chitosan-based bone-targeted nanoparticles delivery of cyclolinopeptide J for the synergistic treatment of osteoporosis. Int J Biol Macromol. 2025;304:140884.
22. Chen J, et al. The synergistic treatment of cyclolinopeptide J and calcium carbonate nanoparticles for osteoporosis via BMP/Wnt signaling: in vivo and in vitro. J Funct Foods. 2023;110:105826.

23. Liu X, et al. A practical and fast isolation of 12 cyclolinopeptides (linusorbs) from flaxseed oil via preparative HPLC with phenyl-hexyl column. Food Chem. 2021;351:129318.
24. Liu L, et al. Cyclicpepedia: a knowledge base of natural and synthetic cyclic peptides. Brief Bioinform. 2024;25(3):bbae190.
25. Abdelkarem HM, Abd El-Kader MM, Kasem SA. Manipulation of flaxseed inhibits tumor necrosis factor-alpha and interleukin-6 production in ovarian-induced osteoporosis. Saudi Med J. 2011;32(4):369–75.
26. Kverka M, Stepan JJ. Associations among estrogens, the gut microbiome and osteoporosis. Curr Osteoporos Rep. 2024;23(1):2.
27. Sacco SM, et al. Accessibility of 3H-secoisolariciresinol diglycoside lignan metabolites in skeletal tissue of ovariectomized rats. J Med Food. 2011;14(10):1208–14.
28. Tang C, et al. Omentin–1 induces osteoblast viability and differentiation via the TGF–β/Smad signaling pathway in osteoporosis. Mol Med Rep. 2022;25(4):132.
29. Ponzetti M, Rucci N. Osteoblast differentiation and signaling: established concepts and emerging topics. Int J Mol Sci. 2021. https://doi.org/10.3390/ijms22136651.
30. Wan Hasan WN, et al. Annatto-derived Tocotrienol stimulates osteogenic activity in preosteoblastic MC3T3-E1 cells: a Temporal sequential study. Drug Des Devel Ther. 2018;12:1715–26.
31. Kaneda T, et al. Cyclolinopeptides, cyclic peptides from flaxseed with osteoclast differentiation inhibitory activity. Bioorg Med Chem Lett. 2016;26(7):1760–1.
32. Kaneda T, et al. Cyclolinopeptide F, a cyclic peptide from flaxseed inhibited RANKL-induced osteoclastogenesis via downergulation of RANK expression. J Nat Med. 2019;73(3):504–12.
33. Yang X, et al. The role and mechanism of SIRT1 in Resveratrol-regulated osteoblast autophagy in osteoporosis rats. Sci Rep. 2019;9(1):18424.
34. Fu Y, et al. LncRNA ROR/miR-145-5p axis modulates the osteoblasts proliferation and apoptosis in osteoporosis. Bioengineered. 2021;12(1):7714–23.
35. Kim J-M, et al. Osteoblast-osteoclast communication and bone homeostasis. Cells. 2020. https://doi.org/10.3390/cells9092073.
36. Zhou L, et al. ATP-binding cassette G1 regulates osteogenesis via Wnt/β-catenin and AMPK signaling pathways. Mol Biol Rep. 2020;47(10):7439–49.
37. Chandra A. Skeletal aging and osteoporosis: mechanisms and therapeutics. Int J Mol Sci. 2021. https://doi.org/10.3390/ijms22073553.
38. Cheng C-H, Chen L-R. *Osteoporosis* due to hormone imbalance: an overview of the effects of Estrogen deficiency and glucocorticoid overuse on bone turnover. Int J Mol Sci. 2022. https://doi.org/10.3390/ijms23031376.
39. Ma Y, et al. Cadmium exposure triggers osteoporosis in duck via P2X7/PI3K/AKT-mediated osteoblast and osteoclast differentiation. Sci Total Environ. 2021;750:141638.
40. Abdurahman A, et al. Loading-driven PI3K/Akt signaling and erythropoiesis enhanced angiogenesis and osteogenesis in a postmenopausal osteoporosis mouse model. Bone. 2022;157:116346.